A. Boev, R. Bregovic, D. Damyanov, and A. Gotchev, "Anti-aliasing filtering of 2D images for multi-view auto stereoscopic displays," *Proc. 2009 Int. Workshop on Local and Non-Local Approximation in Image Processing*, Tuusula, Finland, Aug. 2009, pp. 87–97.

ANTI-ALIASING FILTERING OF 2D IMAGES FOR MULTI-VIEW AUTO-STEREOSCOPIC DISPLAYS

Atanas Boev[1], *Robert Bregovic*[1], *Damyan Damyanov*[2], *and Atanas Gotchev*[1]

[1] Department of Signal Processing, Tampere University of Technology, Finland,
[2] Department of Telecommunications, Technical University of Sofia, Bulgaria
[1] firstname.lastname@tut.fi, [2] ellov@abv.bg

ABSTRACT

Abstract – In this paper, we address the problem of anti-aliasing filtering of images to be displayed on auto-stereoscopic displays. Auto-stereoscopic displays are constructed to create 3D visual effect by no special glasses but utilizing extra optical layer to cast different images to different directions. The topology of such layer is a compromise between the number of different views generated and the spatial resolution per view being fraction of the full 2D spatial resolution. Usually, the compromise is achieved by slanted and non-rectangular sub-sampling grids causing however corresponding aliasing artefacts. These artefacts are especially visible and annoying when 2D imagery, such as graphics and text, is to be displayed on auto-stereoscopic displays. In our work, we design efficient anti-aliasing filters to mitigate this effect. Two classes of filters are studied for a 3D display case. The first class is the class of non-separable filters, which takes into account the non-rectangular topology of the particular sub-sampling grid and the effect of inter-view crosstalk, and aims at suppressing the respective aliasing replicas appearing in non-rectangular positions on the 2D Fourier plane. The second class is the class of efficient separable 2D filters based on 1D anti-aliasing filter design. We demonstrate that the latter class results in subjectively higher quality images. Studying this particular case further, we design filters for different types of imagery, distinguishing between text and graphics and also between 'smooth' and 'sharp' target anti-aliased images. As it is difficult to quantify the results by objective measures, we illustrate them by visual examples. Subjective inspections have also confirmed the feasibility of our approach.

1. INTRODUCTION

3D displays aim at delivering the perception of depth (the third dimension). Certain types of 3D displays recreate 3D scenes without requiring the observer to wear special glasses. Such 3D displays are known as auto-stereoscopic displays, and they work by casting two or more different images each one visible from different angle. Due to this principle of operation, only a subset of all image pixels is visible from a particular angle. The visible pixels appear on a non-rectangular grid, and rendering images on this grid requires special anti-aliasing filters [1], [2].

A 3D display may be used to visualise a combination of 2D and 3D objects, or 2D content only, if 3D content is not available. In a mixed scene, aliasing artefacts are especially visible in 2D objects [1], [4]. Our work studies two sets of filters, which can be used for anti-aliasing of such content.

The paper is organized as follows: the next section briefly explains how multi-view displays work, and how its optical characteristics can be measured and modelled. Results for a particular multi-view display – namely 23" X3D produced by NewSight – are given as example. Sections 3 and 4 present two different approaches in designing anti-aliasing filters optimized for a specific 3D display. In Section 3, optical measurements of grid topology and interview crosstalk are used for designing non-separable 2D anti-aliasing filter for the 23" X3D display, while Section 4 presents an attempt to reproduce the same results using separable filters. Different filters are proposed for "image" and "text only" 2D content.

Finally, the visual quality and computational intensity of different anti-aliasing filters is compared in Section 5. Both simulated images and snapshots of 23" X3D display showing different test images are given as example.

2. MULTIVIEW DISPLAYS

2.1. Principles of operation

Modern multi-view displays use TFT matrix for image generation [1], [5], [6]. An optical filter is mounted on the surface of the display as shown in Figure 1a. The filter redistributes the light coming from the TFT towards different horizontal directions.

The set of sub-pixels, visible from given direction form a colour image, also known as a *view*. The range of angles, from which a view can be seen, is known as the *visibility zone* of that view. Usually, the visibility zones of all views appear in horizontal direction in front of the display, as depicted in Figure 1b.

In order to visualize a scene in 3D, a number of different observations of that scene should be simultaneously shown on the 3D display. The process of mapping an image to the sub-pixels corresponding to one view is called *view interleaving* or *view interdigitation* [1]. The map of correspondences between addressable sub-pixels

of the display and the view they belong to is called *interdigitation map*. Usually the interdigitation map has repetitive structure, which can be represented by an *interdigitation pattern* copied multiple times over the display surface.

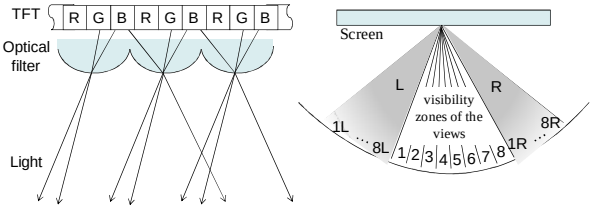

a) b)

Figure 1. Operation principles of a multi-view display: a) optical filter (view from the top) and b) visibility zones of the views (view from the top)

When 3D object is visualized on a multi-view display with *n* views, *n* different observations are interleaved into one compound 3D image. A 2D object, which is not meant to appear floating in front or behind the screen surface, is represented by *n* identical observations. In this case, the optical filter can be regarded as a mask, which partially covers the underlying 2D image.

2.2. NewSight 23" X3D multi-view display

The multi-view display studied in this paper is *23" 3D-Display AD* built by X3D-Technologies GmbH. The display uses 23" TFT monitor with resolution of 1920x1200. The display area is 495x310mm and the optimal distance for observing the 3D effect is 1.5m. The X3D display is marketed as 8 view 3D display with interdigitation pattern as shown in Figure 2a [7].

	Column 1			Column 2			Column 3		
row	r	g	b	r	g	b	r	g	b
1	1	2	3	4	5	6	7	8	1
2	2	3	4	5	6	7	8	1	2
3	2	3	4	5	6	7	8	1	2
4	3	4	5	6	7	8	1	2	3
5	4	5	6	7	8	1	2	3	4
6	4	5	6	7	8	1	2	3	4
7	5	6	7	8	1	2	3	4	5
8	6	7	8	1	2	3	4	5	6
9	6	7	8	1	2	3	4	5	6
10	7	8	1	2	3	4	5	6	7
11	8	1	2	3	4	5	6	7	8
12	8	1	2	3	4	5	6	7	8

a)

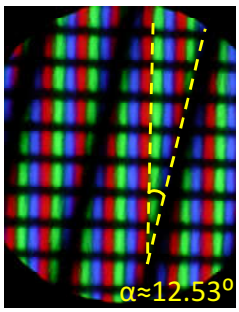

b)

Figure 2. X3D 23" display: a) interdigitation pattern, b) micrograph of the optical filter

The optical filter is called *wavelength-selective filter array* [5], which works similarly to a parallax barrier – blocking the light in some directions and passing light in others. The filter array has regular structure, mounted on the display at a slant of 12.53 degrees, as can be seen from the micrograph in Figure 2b.

Following the interdigitation pattern, one can construct a map of sub-pixels visible from certain angle – for example the sub-pixels marked with "1" in Figure 3a. For different observation angles the map of visible sub-pixels is the same, only shifted in horizontal and vertical direction.

2.3. Crosstalk

Multi-view displays suffer from two common artefacts - *image flipping*, caused by the noticeable transition between the viewing zones, and *picket fence effect*, caused by optical filter magnifying the gaps between sub-pixels. The common practice to mitigate this effect is to broaden the observation angle of each view, thus interspersing the visibility zones [5]. As a result, from a particular angle, a number of views are simultaneously seen. The view originally intended to be seen is the brightest one, but its neighbouring view are visible as well. This effect can be regarded as inter-channel crosstalk.

Methodology for crosstalk estimation and measurement results for 23" X3D were presented in [4]. Based on these measurements the optical masking pattern is reconstructed as shown in Figure 3b. The masking pattern defines the set of sub-pixels visible on the display from a particular direction, as well as their relative brightness in the range between 0 (black) to 1 (maximum brightness).

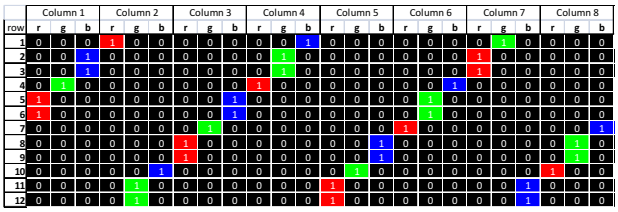

a)

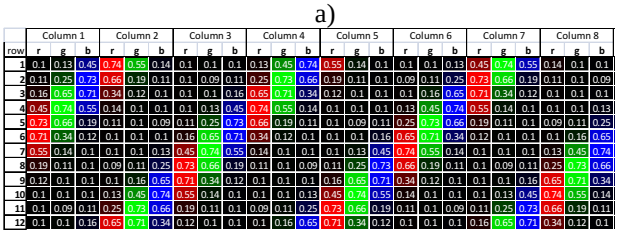

b)

Figure 3. Map of visible sub-pixels from a particular angle: a) without crosstalk, b) with crosstalk

2.4. Aliasing

Selective masking of a 2D image caused by optical filter can be modelled as a sub-sampling on a non-orthogonal grid. Without pre-filtering this process creates aliasing artefacts.

An example for aliasing artefacts on 23" X3D display is given in Figure 4, where simulated image is shown next to an actual photograph of the display. The original 2D image can be seen in Figure 20a. Aliasing process is simulated by using the sub-pixel visibility map from Figure 3a as a mask. The masked image, shown in Figure 4a exhibits noticeable aliasing artefacts. Alternatively, the 2D image was visualized on the 23" X3D display and a photo was taken. The photographed image is shown in Figure 4b.

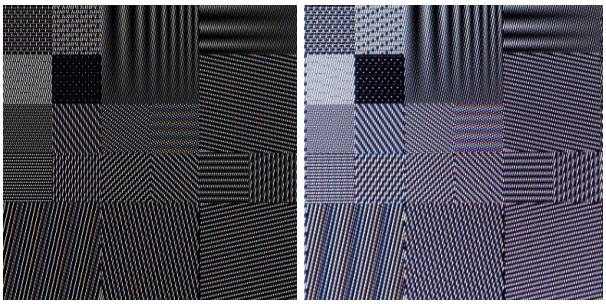

a) b)

Figure 4. Aliasing, caused by optical filter: a) simulated image (fragment) and b) actual photograph of the X3D display (fragment). The original image used for the experiment is shown in Figure 20a

In multi-view displays aliasing artefacts appear in all types of scenes, but are especially visible in 2D content, as in 3D images aliasing is somewhat masked by more severe artefacts such as ghosting [1][4]. While most of content created for multi-view display would be in 3D, there are cases where 2D images would appear on such display as well. The typical cases include 2D graphics, 2D text and natural 2D images.

In order to eliminate aliasing errors due to the non-orthogonal sub-sampling pattern of the display, in this paper two different methods for designing anti-aliasing filters have been applied. The first one is based on non-separable filters and the second one on separable ones. These methods are discussed in detail in the following two sections.

3. NON-SEPARABLE ANTIALIASING FILTERS

First method for designing anti-aliasing filters is based on the method introduced by Jain and Konrad in [1] (in the rest of the paper it will be referred to as the JK method). JK method can be used for designing 2D non-separable anti-aliasing filters for an arbitrary sub-sampling pattern. It is assumed that a 2D image is processed and correspondingly, the method works best for 2D imagery.

The basic idea of the JK method is to design a 2D filter in such a way that the passband of the filter spans all frequencies at which the contribution of all alias terms is smaller than the original signal itself. The stopband of the filter is assumed to span all other frequencies. This is achieved by the following steps: First, based on the sub-sampling pattern the position and intensity of all aliasing terms in the 2D frequency domain is estimated. Second, the contribution of these aliasing terms to the overall spectrum of a given image is evaluated. Instead of using a particular image, an image model is utilized. In [1], the use of a first-order 2D Markov model is suggested for modelling the image. Third, the passband of the ideal filter is selected as the region where the spectrum of the signal is greater than the contribution of all aliasing terms. The rational for this is that all frequencies should be preserved for which the signal is stronger than the aliasing terms. Finally, fourth, a filter design technique is applied to design the filter itself based on the above determined specifications.

In [1], the JK method has been applied for the 9-view SynthaGram SG202 monitor. In our work, we reproduce their approach for the case of the X3D display under consideration. We specifically utilize our measurements of the grid topology and the inter-view crosstalk obtained for that display. We consider two cases: crosstalk free case and crosstalk-aware case. The first case assumes that the viewer can see, while at an observing position corresponding to a certain view, pixels belonging to that view only. In the crosstalk-aware case, it is assumed that the viewer can see, in addition to the pixels from the principal view, also pixels from the adjacent views.

3.1. Crosstalk-free case

In this case the display is considered ideal, that is, no interference between neighbours channels exist. For an ideal display with n views the viewer sees only $1/n$ pixels of the display, or, roughly speaking, about $1/n$ of the whole brightness. Depending on the sub-sampling patterns, in one view a non-uniformly sampled image is seen. Based on the known sub-sampling pattern it is possible to estimate which frequencies in the original image have to be suppressed in order to avoid aliasing.

For the X3D display, the sub-sampling patterns for all colors in all views differ only by a shift in the space domain. There is no difference in the spectral domain. Therefore, in this paper, without loss of generality, when designing filters, the sub-sampling pattern of the red component for the fourth view has been used. This sub-sampling pattern is shown in Figure 5.

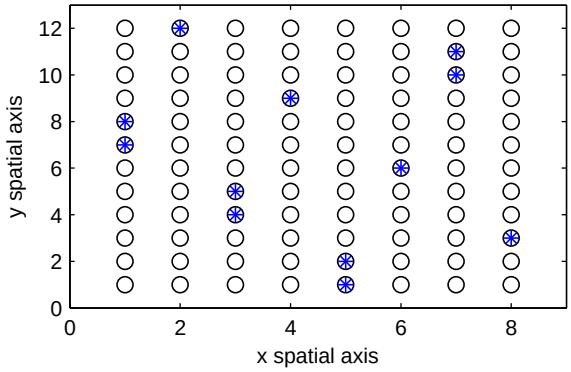

Figure 5. Sub-sampling pattern for the fourth view. Circles and stars represent the orthogonal grid and the sub-sampling pattern, respectively.

The JK method is focused on the non-orthogonal sub-sampling of the image for each view. Taking only one of n points of the image, where n is number of views ($n = 8$ for the X3D display), a significant change in the spectrum of the picture occurs. Essentially, this change can be explained with the occurrence of attenuated replicas of the original spectrum on certain points of the 2D spectral domain. In the well known case of a sampled 1D signal, replications of the original spectrum occur on points,

which are equal to the integer multipliers of the sampling frequency. In the 2D case with non-orthogonal sampling the replicas occur on various positions depending on the sub-sampling pattern. For the sub-sampling pattern given by Figure 5, the position and amplitude of the main spectral component and all replicas are shown in Figure 6. The main spectral component (baseband spectrum) is located at $(f_x, f_y) = (0, 0)$. All other peaks represent positions of spectrum replicas.

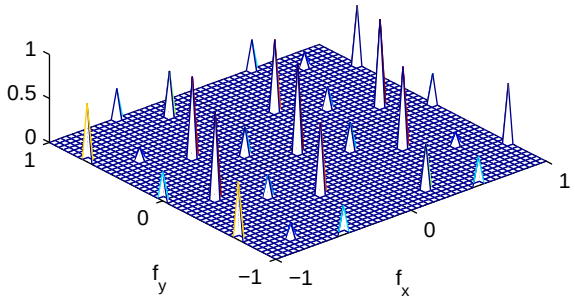

Figure 6. Spectrum of the sub-sampling pattern for the fourth view.

In order to determine the contribution of all alias terms independent of the image itself, a statistical representation of a real image has been used. As in [1], a 2D separable autocorrelation model $R_u[m,n] = \rho^{|m|}\rho^{|n|}$ has been utilized. Here, $0 < \rho < 1$ is the correlation coefficient and is typical chosen in the 0.9-0.99 range. This model is based on the first-order Markov model as discussed in [1], [9]. The power spectral density of this autocorrelation model is:

$$\Phi(f_x, f_y) = \frac{1}{\pi^2}\frac{f_0^2}{(f_x^2 + f_0^2)(f_y^2 + f_0^2)}, \qquad (1)$$

with $f_0 = -(\ln\rho)/(2\pi)$ and f_x and f_y being the normalized frequencies. The power spectral density function for $\rho = 0.9$ is shown in Figure 7.

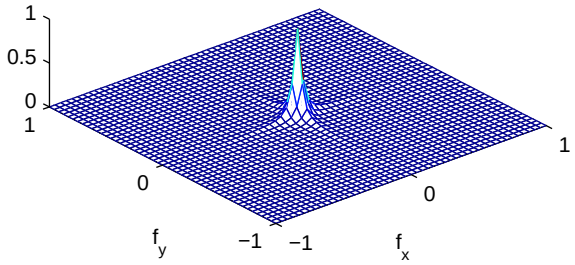

Figure 7. Power spectrum density function for the used autocorrelation model with $\rho = 0.9$.

In terms of classical anti-aliasing theory one should take the original spectra and try to suppress all other replicas in order to obtain an alias-free signal. In practice, this would be too restrictive. Therefore, in the JK method a different approach is used. The idea is to widen the passband of the anti-aliasing filter as much as possible. This can be done by defining the boundary of the passband as follows: The cut-off frequencies of the filter are set at points where the amplitude of the original spectrum equals to the sum of all amplitudes of the spectral replicas. This can be formulated as:

$$H_d(f_x, f_y) = \begin{cases} 1, \ if \ \Phi(f_x, f_y) > K\sum_i \beta_i \Phi(\xi_x^i - f_x, \xi_y^i - f_y) + \varepsilon \\ 0, \quad \text{otherwise} \end{cases} \qquad (2)$$

The variables (f_x, f_y) represent the spectral coordinates across x and y spectral axis, respectively. H_d is the desired frequency response of the anti-aliasing filter, (ξ_x^i, ξ_y^i) are the coordinates along x and y axis at which the i-th spectral replica occurs and β_i is its associated gain. The constant K perzmits changes in the pass-band of the filter. In this paper $K = 1$ has been used. Finally, ε is used to eliminate some regions in corners of the spectrum that due to the used image model could be declared as passbands. In this paper, for all designs, $\varepsilon = 0.001$ has been used.

By evaluating Equation (2), the desired frequency response of the ideal 2D filter $H_{id}(f_x, f_y)$ is shown in Figure 8. For designing a 2D filter approximating this ideal one, the widowing method with the Hamming window of length $N = 49$ has been used (for more detail see `fwind2` function in Matlab). The impulse response and the magnitude response of the designed filter are shown in Figure 9 and Figure 10, respectively. As seen on Figure 3a, only 1/8th of the available pixels are visible in one view. Therefore it is to expect that the passband area of the filter should be approximately 1/8. However, the passband surface of the filter designed for the crosstalk-free case is considerably smaller – 0.037. This proves that assuming crosstalk-free view model is too restrictive for the given visibility map. Therefore in the next section the contribution of adjacent views is taken into account.

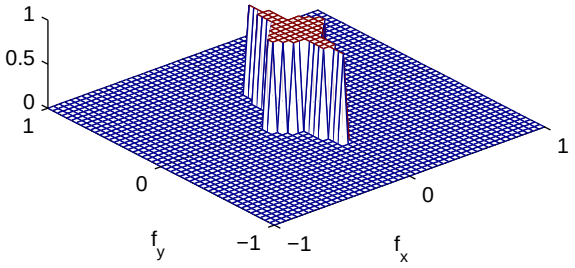

Figure 8. Magnitude response of the ideal filter in the cross-talk case.

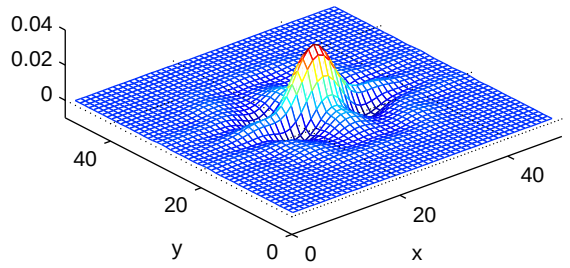

Figure 9. Impulse response of the filter in the crosstalk-free case.

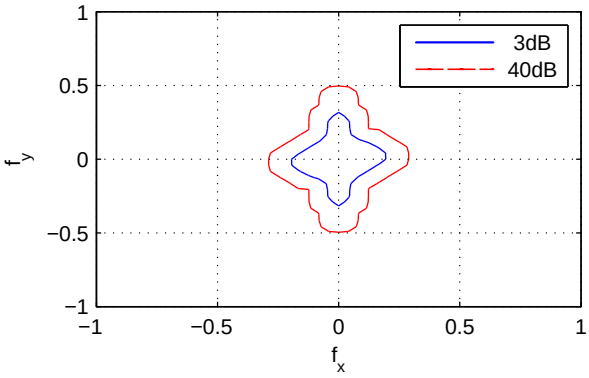

Figure 10. Magnitude response (contour) of the filter in the crosstalk-free case.

3.2. Crosstalk-aware case

In the previous section, it was assumed that in one view only pixels from that view are seen. In practice, as it has been experimentally observed [1], [4], that in addition to pixels from the view under consideration, pixels from adjacent views are also visible, although with a smaller intensity. For the display under consideration, the sub-sampling pattern for fourth view with contributions from the adjacent third and fifth view is shown in Figure 11. It has been measured that the contributions of those three views are, in average, as shown in Table I.

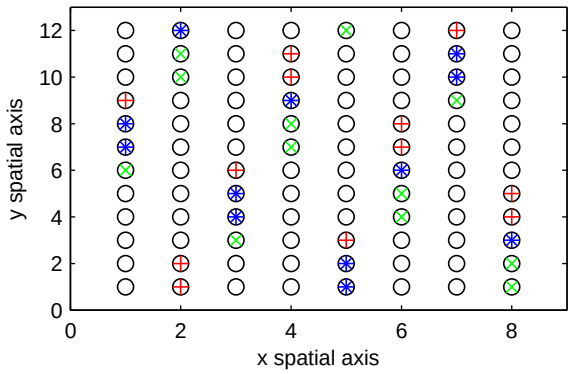

Figure 11. Sub-sampling pattern for the fourth view with contributions from the third and fifth view. Circles represent the orthogonal grid. Stars (blue), pluses (red) and x (green) are the sub-sampling patterns for fourth, third and fifth view, respectively.

Table I Contributions of individual views to the fourth view

View	#3	#4	#5
Amplitude	0.43	1.00	0.43

For this sub-sampling pattern, the spectrum is shown in Figure 12. Again, the term at $(f_x, f_y) = (0, 0)$ corresponds to the original, non-aliased term. It can be observed that the position of aliasing terms is the same as for the crosstalk-free case. However the contribution (amplitude) of each alias component is smaller than in the crosstalk-free case. This can be interpreted that due to the crosstalk more of the image is seen in one view and as such the overall aliasing is smaller.

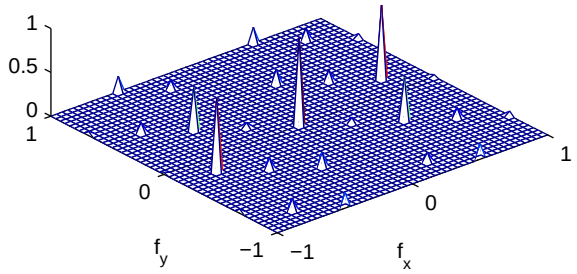

Figure 12. Spectrum of the sub-sampling pattern for the fourth view with contributions from third and fifth view.

By applying the same procedure as discussed in the previous section, specifications for the ideal filter can be determined. This ideal filter is shown in Figure 13. The impulse response and the magnitude response of the designed filter are shown in Figure 14 and Figure 15, respectively. The passband surface of the ideal filter is 0.068. This is still less than 1/8. It can be concluded that both crosstalk-free and crosstalk-aware filters are too restrictive (this will be also shown in the example section) and as such they are not performing well in practice. Moreover, they are computational heavy. Therefore in the next section a separable filter design is proposed that generates filters that are fast and perform well in practice.

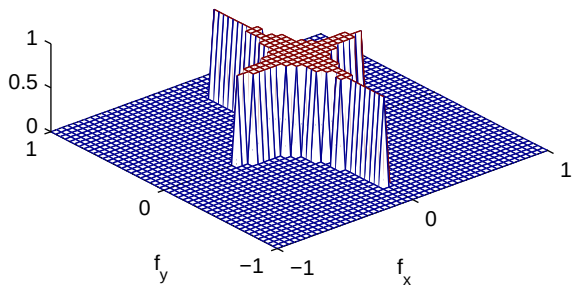

Figure 13. Magnitude response of the ideal filter in the crosstalk case.

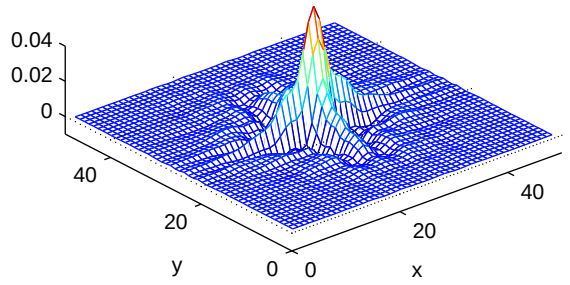

Figure 14. Impulse response of the filter in the crosstalk case.

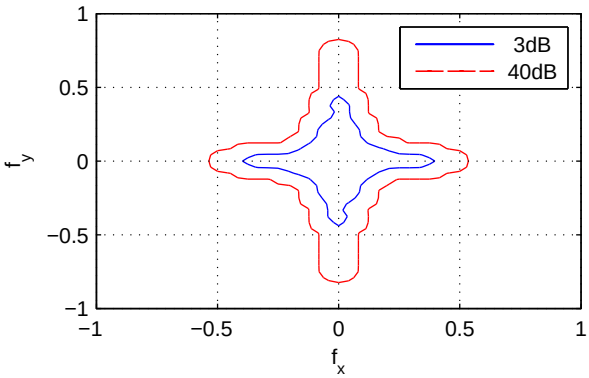

Figure 15. Magnitude response (contour) of the filter in the crosstalk case for attenuations 3 dB and 40 dB.

4. SEPARABLE ANTI-ALIASING FILTERS

In this section a method is proposed for designing separable filters for reducing aliasing errors when showing a 2D image on a 3D screen. The motivation of using separable filters is threefold. First, separable filters are, in principle, easier to design than non-separable 2D filters, second, they are computationally more efficient than non-separable filters of the same size, and, third, by properly designing these filters (allowing some alias errors in the image), visually (subjectively) better results are expected than by using the method described in the previous section.

When using separable filters to filter an image, the image is first filtered in horizontal direction and then, in some cases, in vertical one. This will be referred to as the horizontal and vertical filtering. Parameters related to horizontal and vertical filters will be denoted by subscript *h* and *v*, respectively. Consequently, instead of one 2D filter, two 1D FIR filters have to be designed.

4.1. 1D filter design

There are many methods for designing FIR filters. When selecting a design method to be used in this paper, following two criteria were taken into account: First, the method has to be fast because many filters had to be designed in order to choose the best one for the given problem. Second, the filters should have enough attenuation in the stopband in order to suppress aliasing terms. A good candidate satisfying the above two conditions are FIR filters designed in the least-mean-square (LMS) sense [10]. In this filters the energy of the error in stopband and passband is minimized. The design problem for an FIR filter with transfer function

$$H(z) = \sum_{n=0}^{N} h[n] z^{-n} \qquad (3)$$

can be stated as follows: For a given filter order N, passband and stopband edges ω_p and ω_s minimize

$$E_2 = \int_0^{\omega_p} \left(H(e^{j\omega}) - e^{-j\omega N/2} \right)^2 d\omega + \int_{\omega_p}^{\pi} H(e^{j\omega})^2 d\omega . \qquad (4)$$

After some mathematical manipulations, the above problem can be rewritten as

$$E_2 = \boldsymbol{h}^T \boldsymbol{Q} \boldsymbol{h} + \boldsymbol{h} \boldsymbol{b} + c . \qquad (5)$$

Here, $\boldsymbol{h}$ is the vector containing the filter coefficients, and $\boldsymbol{Q}$ and $\boldsymbol{b}$ are a matrix and a vector that depend only on the filter order and passband and stopband edges and c is a constant [10]. The energy of the error is minimized for

$$\boldsymbol{h} = \boldsymbol{Q}^{-1} \boldsymbol{b} , \qquad (6)$$

that is, in order to design a filter for a given N, ω_p, and ω_s, only a system of linear equations has to be solved. Moreover, the energy in the stopband is minimized, which in turn, minimizes the aliasing error. Therefore, both of the initial criteria are taken care of.

Due to the non-orthogonal sampling pattern, it is not easy to decide what values for filter order, passband and stopband edges should be selected. Therefore, subjective experiments have been performed to determine good values of these parameters. The experiments have been carried out by using the following steps:

Step 1. An appropriate image has been selected.

Step 2. The initial filter orders, passband edge and stopband edge were selected as $N_h = 30$, $\omega_{ph} = 0.8$, $\omega_{sh} = 0.9$, $N_v = 30$, $\omega_{pv} = 0.8$, $\omega_{sv} = 0.9$. The motivation of choosing these parameters lies in the fact that the difference between images filtered with such filters and non-filtered images, when seen on the X3D display, is negligible. As the goal is to improve the images after filtering, this turned out to be a good starting point.

Step 3. First, edges ω_{ph} and ω_{sh}, and then, filter order N_h were reduced until an image of satisfied quality (described in more detail in following sections) is achieved. As this parameters influence filtering in the horizontal direction, only features containing vertical lines (and ones close to vertical) have be considered during this step. The

minimal values for parameters N_h, ω_{ph}, and ω_{sh} are considered to be the optimal ones.

Step 4. Keeping the horizontal parameters determined in Step 3, repeat Step 3 by reducing parameters ω_{pv} and ω_{sv} and then filter order N_v. In this case, attention has been paid to horizontal lines and the ones close to them. Again, the minimal values for parameters N_v, ω_{pv}, and ω_{sv} are considered to be the optimal ones.

The above procedure has been repeated three times, twice for an image containing various patterns (patterns have been chosen in such a way to emphasize aliasing errors due to the sub-sampling patterns of the display) and once for text. This is described in the following sections.

4.2. Anti-aliasing of 2D images

For anti-aliasing of 2D images with separable filters, in this paper, two different approaches have been proposed. They will be refereed to as the "smooth" and "sharp" approach and are presented in the following two sections.

4.2.1. "Smooth" approach

In the "smooth" approach the goal was to design filters that will eliminate all alias components from an image. The 4-step procedure described in the previous section has been performed on a test image containing various patterns. The image is shown in Figure 20a. In Steps 3 and 4 of the procedure the parameters have been reduced until all aliasing errors have been suppressed. The parameters for the best filters have been listed in Table II and the filter magnitude responses are shown in Figure 16. The designed filters have relatively small attenuations, but this has turned out to be sufficient. Higher attenuation only increases the filter order but does not improve the image.

Table II Parameters for anti-aliasing filters for images – "smooth" approach

Parameters	N	ω_p	ω_s
Horizontal filter	14	0.22	0.26
Vertical filter	17	0.16	0.20

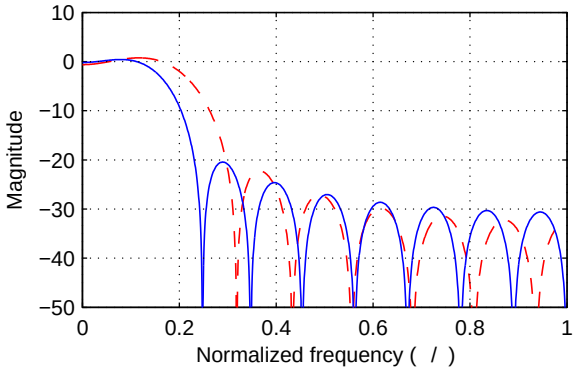

Figure 16. Magnitude response of the horizontal (red dashed line) and vertical (blue solid line) filter for the "smooth" approach.

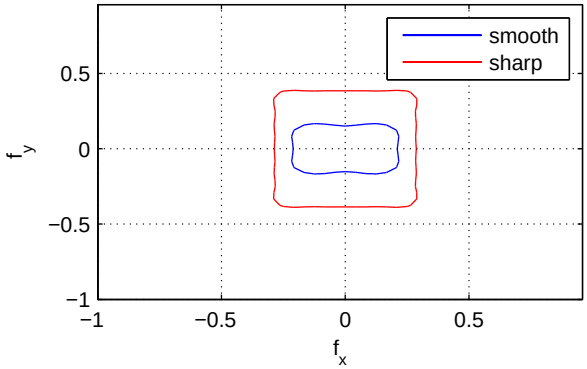

Figure 17. Magnitude response (3dB contour) of the equivalent "smooth" (blue line) and "sharp" (red line) 2D filter.

In order to enable comparison with non-separable filters, in Figure 17 the edges of the passband (3dB point) of an equivalent 2D filter has been shown. The passband surface of this equivalent filter is 0.033.

4.2.2. "Sharp" approach

In the "sharp" approach the goal was to achieve visually good images. Some aliasing was allowed as long as it did not degrade the overall perception of the image. Again, the 4-step procedure described in Section 4.1 has been applied on the image shown in Figure 20a. This time the parameters have been reduced until a 'good' image is obtained. This is highly subjective but as it can be seen in the example section, the selected filters do perform better. The parameters of the best filters are listed in Table III and the filter magnitude responses are shown in Figure 18. The magnitude response (contour) of the equivalent 2D filter has been shown in Figure 17. The passband surface is 0.107. It can be seen that this filter has much wider passband than the non-separable ones as well as the one used for "smooth" approach. After filtering an image with these filters, more details will be preserved but some aliasing will be also visible. However, as it will be illustrated in the example section the gain in image quality is much higher than the visible errors due to aliasing.

It was noticed that the sub-sampling pattern can be approximated by an orthogonal sampling grid rotated clockwise by 12.53 degrees. Based on this fact, it is logically to assume that by rotating the image counter-clockwise by that angle, the sub-sampling pattern would become more regular and as such, more appropriate for filtering. Therefore, in this paper an attempt has been made to do following: First, the image is rotated by 12.53 degrees counter-clockwise. For this purpose, spline-based rotation approach suggested in [8] has been used. Second, the rotated image was filtered with filters designed for the "sharp" approach (parameters are given in Table III). Third, the filtered image has been rotated clockwise by 12.52 degrees. Although, better results were expected, it turned out that filtering rotated or non-

rotated images yield to the same visual result. This can be seen in Figure 20d and Figure 20e.

Table III Parameters for anti-aliasing filters for images – "sharp" approach

Parameters	N	ω_p	ω_s
Horizontal filter	22	0.28	0.33
Vertical filter	22	0.38	0.43

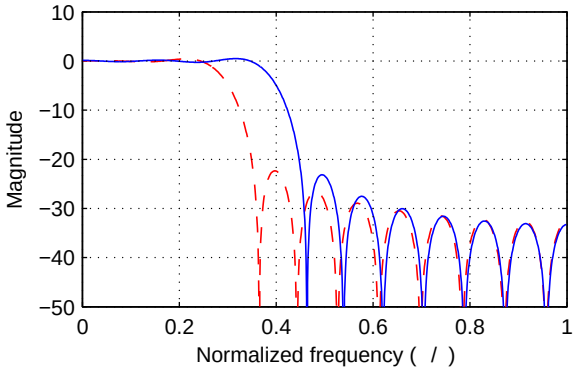

Figure 18. Magnitude response of the horizontal (red dashed line) and vertical (blue solid line) filter for the "sharp" approach.

4.3. Anti-aliasing of text

Text can be considered as a special type of an image. Therefore, same filters can be applied as the one discussed in the previous sections. However, when talking about text, readability is the most important property. It has been shown that people often find over-sharpened text to have better readability. For that reason it is better to design a separate filter for processing text as such filter will have even less anti-aliasing properties, than for example the filters designed in the previous section ("sharp" approach). Moreover, it has been experimentally observed that for text only horizontal filtering is enough. This further simplifies the computational complexity of anti-aliasing filtering. The first 3 steps (Step 4 is not needed as only horizontal filters are used) of the procedure described in Section 4.1 have been applied on an image containing only text. The image is shown in Figure 21a. The parameters for the best filter were selected such that the best readability is achieved. These parameters are given in Table IV with the magnitude response of the filter based on these parameters shown in Figure 19. Two points should be emphasized. First, the passband (3 dB edge) occupies 0.285 of the overall band. This is considerably higher than in the case off all previously introduced filters. Second, the passband ripple of this filter is quite high (almost 1 dB). Nevertheless, this is not a problem because we are processing black and white text. Small changes in the brightness are not affecting the readability. Due to the high passband ripple, smaller filter order can be used.

Table IV Parameters for anti-aliasing filters for text

Parameters	N	ω_p	ω_s
Horizontal filter	12	0.30	0.35

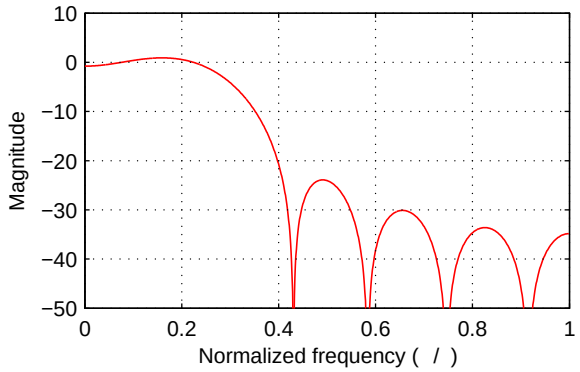

Figure 19. Magnitude response of the horizontal filter for text.

5. RESULTS

Three typical usage scenarios, which result in 2D content being rendered on a 3D display, were identified. Three test images were selected to represent the content in each case. Each image was filtered with different filters, and the results were shown on 23" X3D display and photographed.

The first case is using a 2D graphical user interface to choose or navigate through 3D content. User interfaces contain details with high contrast and straight lines, similar to the "2D graphics" image in Figure 20a. Since the optical filter of 23" X3D is slanted at 12.53 degrees, lines with this orientation are also included in the image. The second case is 2D subtitles being rendered in a 3D movie. This case is represented by the "2D text" test image shown in Figure 21. The "2D text" image contains words with different font sizes and is created using Wordle [11]. The third case is 2D movie being rendered on a 3D display. This is represented by full-colour, natural 2D image. The test image "2D photo" used to test this case is from the Kodak Image Database [12].

In the "2D graphics" tests, there are two groups of filters which produce similar visual results. The first group is filters which remove all aliasing artefacts on expense of over-smoothing the image. The "no crosstalk" non-separable filter (see Figure 20b) and the "smooth" set of separable filters (Figure 20f) fall in this group. The other group is filters which produce sharper image, preserve more details, but leave some aliasing in the image. The "crosstalk aware" non-separable filter (see Figure 20c) and the "sharp" ser of separable filter (Figures 5d and 5e) are in this category. Notably, there is negligible visual difference when applying separable fitters with or without rotation.

In the "2D text" tests, the "text optimized" separable filter produces results with highest readability, as seen in

Figure 21d, outperforming the "no crosstalk" and "crosstalk aware" non-separable filters. Finally, in the "2D photo" tests the "sharp" set of separable filters produces best visual results, closely followed by the "crosstalk aware" non-separable filter.

It can be seen from the figures that visually the images filtered by the proposed separable filters are considerably better than the one filtered by the 2D filters. Beside this, filtering images with separable filters is also more computationally efficient. In order to illustrate this, in Table V the computational complexity for various filters discussed in this paper are given. As it can be seen, the non-separable filters of size N by N have complexity proportional to N^2, whereas the separable ones of order N have the complexity proportional to N.

Table V Computational complexity for various filters discussed in this paper. *C* stands for required number of multiplication per pixel.

Filter type		Filter size	*C*
2D non-separable	one view	48 by 48	2304
	crosstalk	48 by 48	2304
2D separable	"smooth"	15 and 18	43
	"sharp"	23 and 23	46
1D	text	13	13

6. CONCLUSIONS

Different methodologies for design of anti-aliasing filters for multi-view displays were presented. The filters were optimized for 2D content, which is most affected by aliasing artefacts. Two separable and three non-separable anti-aliasing filters were compared for three types of typical 2D content. The effect of the filters was demonstrated on an actual multi-view 3D display. The results show, that specially optimized separable filters can produce similar or better visual results that non-separable ones, while requiring much less computational operations per pixel.

7. ACKNOWLEDGMENTS

This work is partially supported by the European Commission within the ICT Programme of FP7 under Grant 216503 with the acronym MOBILE3DTV.

8. REFERENCES

[1] A. Jain and J. Konrad, "Crosstalk on automultiscopic 3-D displays: Blessing in disguise?," in *Proc IS&T/SPIE Symposium on Electronic Imaging, Stereoscopic Displays and Applications*, San Jose, CA, Vol. 6490, pp. 649012 (2007).

[2] M. Zwicker, W. Matusik, F. Durand, H. Pfister, "Antialiasing for Automultiscopic 3D displays", In *Proc. of Eurographics Symposium on Rendering*, Cyprus, 2006

[3] S. Pastoor, "3D displays", in (Schreer, Kauff, Sikora, edts.) *3D Video Communication*, Wiley, 2005.

[4] A. Boev, A. Gotchev and K. Egiazarian, "Crosstalk measurement methodology for auto-stereoscopic screens", *in Proc. of 3DTV Con*, Kos, Greece, 2007

[5] C. Van Berkel and J. Clarke, "Characterisation and optimisation of 3D-LCD module design", *in Proc. SPIE Vol. 2653, Stereoscopic Displays and Virtual Reality Systems IV*, (Fisher, Merritt, Bolas, edts.), p. 179-186, May 1997

[6] A. Schmidt and A. Grasnick, "Multi-viewpoint autostereoscopic displays from 4D-vision", *in Proc. SPIE Photonics West 2002: Electronic Imaging*, vol. 4660, pp. 212-221, 2002.

[7] X3D-23" Users' Manual. NewSight GmbH. Firmensitz Carl-Pulfrich-Str. 1 07745 Jena, 2006

[8] M. Unser, P. Thevenaz, and L. Yaroslavsky, "Convolution-based interpolation for fast, high-quality rotation of images", *IEEE Trans. Signal Processing*, vol. 4, pp. 1371-1381, 1995.

[9] A. Jain, *Fundamentals of Digital Signal Processing*, Information and System Science Series, Prentice Hall, 1989.

[10] S. K. Mitra, *Digital signal processing: A computer based approach*, New York: McGrow-Hill, 2005

[11] Wordle, online tool for generating "word clouds", available online at http://www.wordle.net

[12] Kodak image database, available online at ftp://ftp.kodak.com/www/images/pcd

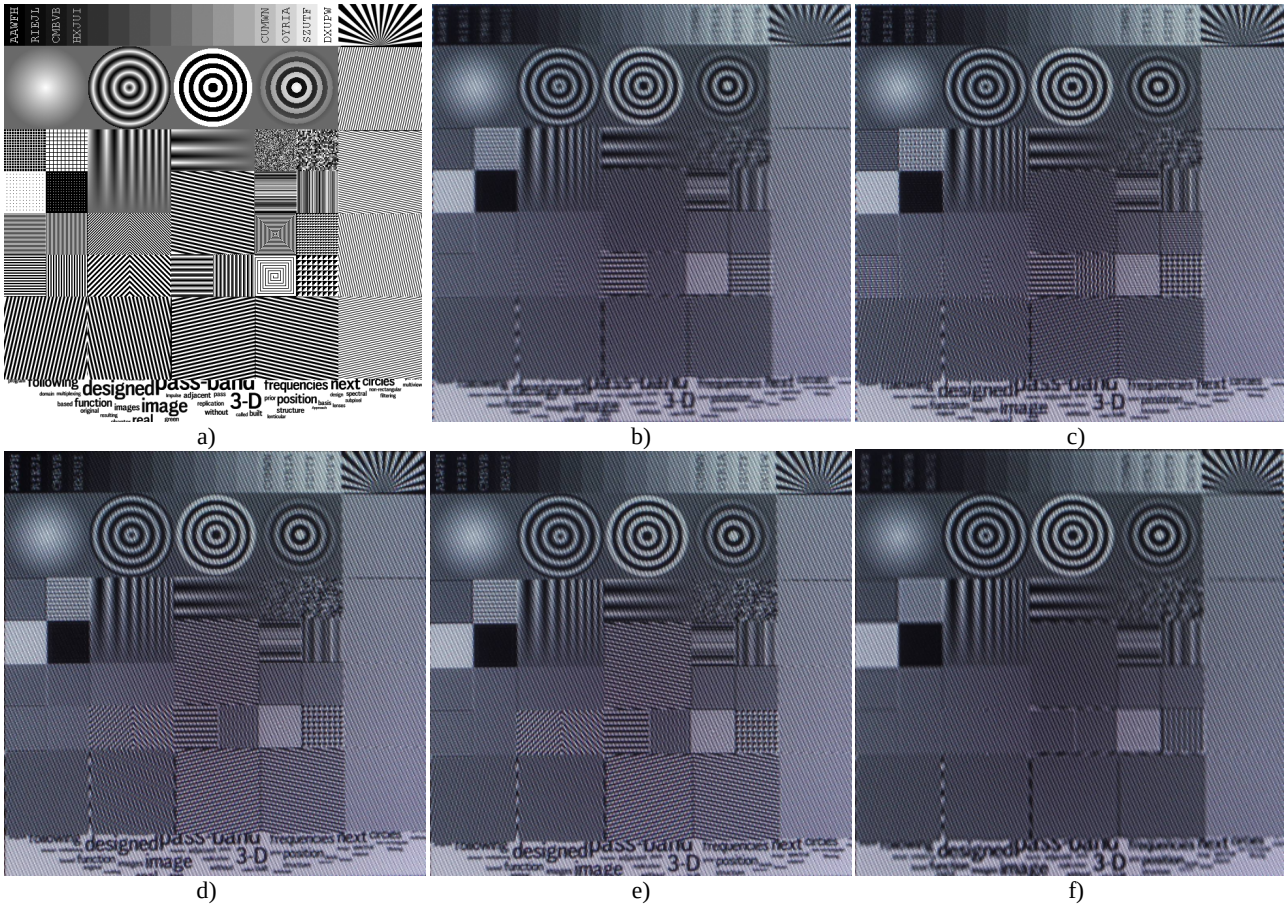

a) b) c)

d) e) f)

Figure 20, “2D graphics” test case: a) original image, b)-f) photographs of the display, as follows – b) filtered with non-separable filter without taking crosstalk into account, c) filtered with non-separable filter taking crosstalk into account, d) filtered with “sharp” set of separable filters after rotation, e) filtered with “sharp” set of separable filters without rotation, and f) filtered with “smooth” set of separable filters without rotation

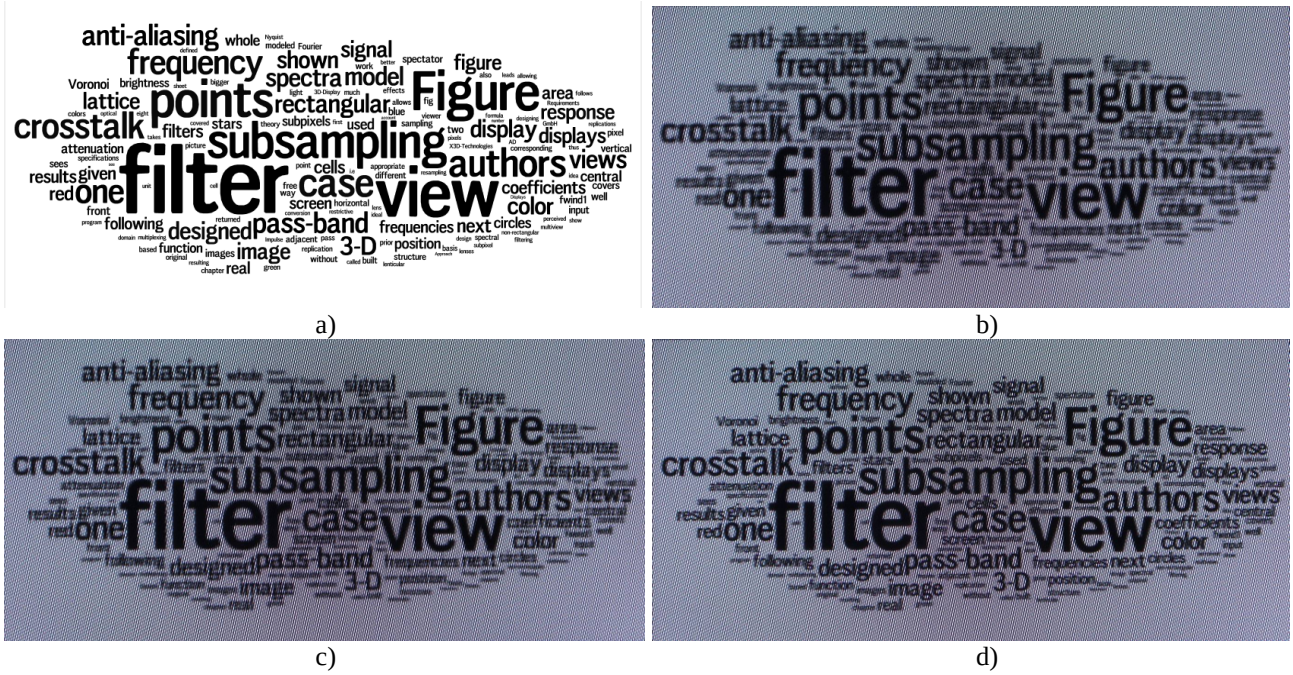

a) b)

c) d)

Figure 21, “2D text” test case: a) original image, , b)-d) photographs of the display as follows – b) filtered with non-separable filter without taking crosstalk into account, c) filtered with non-separable filter taking crosstalk into account, and d) filtered with set of separable filters optimized for text, without rotation

a) b) c)

d) e) f)

Figure 22, “2D photo” test case on multi-view display: a) original images, b)-f) photographs of the display, as follows – b) without filter, exhibiting crosstalk, c) filtered with non-separable filter without taking crosstalk into account, d) filtered with non-separable filter taking crosstalk into account, e) filtered with “sharp” set of separable filters without rotation, and f) filtered with “smooth” set of separable filters without rotation